MAUSAM, **72**, 1 (January 2021), 237-252

551.515.2 : 551.509.313

Synoptic and dynamical characteristics of super cyclone Amphan

PRAVAT RABI NASKAR and SOMNATH NASKAR*

Meteorological office Port Blair, India Meteorological Department,

Ministry of Earth Sciences – 744 106, Port Blair, India

**Department of Industrial Engineering,*

Maulana Abul Kalam Azad University of Technology – 700 064, Kolkata, India

e mail : pravat091@gmail.com

सार – यह अध्ययन उष्णकटिबंधीय चक्रवात अम्फन की उत्पत्ति और उसके तीव्रीकरण में मदद करने वाले सिनॉप्टिक और गतिशील परिस्थितियों का पता लगाने के लिए किया गया है। ऐसा देखा गया है कि समुद्र सतह के उच्च तापमान की अनुकूल परिस्थितियों, उच्च ऊर्जा और क्षैतिज पवन के क्षीण उर्ध्वाधर अपरूपण से, 200 हेक्टा पास्कल STWJ से अम्फन की उत्पत्ति में मदद मिली है। क्षीण ऊर्ध्वाधर अपरूपण, गर्म समुद्र सतह और ठंडे वायुमंडल और प्रबल ऊपरी स्तर के विचलन के बीच उच्च तापमान ढाल ने समुद्र की सतह और वातावरण के बीच गर्मी और नमी के आदान-प्रदान को सतह की गर्मी के प्रवाह और ऊर्ध्वाधर हवाओं के माध्यम से बढ़ा दिया और इस प्रणाली ने संवहन और तीव्रता को बढ़ाया। समुद्री सतह का असामान्य उच्च तापमान (17 मई को), और प्रबल ऊपरी-स्तरीय विचलन, निचले स्तर के अभिसरण और निम्न पवन अपरूपण के संयुक्त प्रभाव के कारण अम्फन के तेजी से तीव्रीकरण का कारण हो सकता है। 400 हेक्टा पास्कल द्रोणी के साथ अंत: क्रिया ने भी अम्फन को तीव्र कर दिया। इस द्रोणी और ऊपरी स्तर के जेट ने अम्फन के प्रक्षेप पथ को दिशा दिखाई।

ABSTRACT. This study has been undertaken to find out the synoptic and dynamical conditions those have helped in the genesis and intensification of tropical cyclone Amphan. It has been found that, under favourable conditions of high SST, high energy and weak vertical shear of horizontal wind, the 200 hPa STWJ has helped in the genesis of Amphan. The weak vertical shear, the high-temperature gradient between warmer sea surface & colder atmosphere and strong upper-level divergence has increased the heat and moisture exchange between the sea surface and the atmosphere *via* surface heat fluxes and vertical winds and enhanced the convection and intensified the system. Abnormally high SST (on 17^{th} May) and combined effect of strong upper-level divergence, lower level convergence and low wind shear may be the reason behind the rapid intensification of Amphan. The interaction with 400 hPa trough has also intensified Amphan. This trough and upper-level jet have guided Amphan in its trajectory.

Key words – Amphan, Super cyclone, STWJ, Surface sensible heat flux, Surface latent heat flux, Genesis, ERA5.

1. Introduction

Tropical cyclones are one of the most notorious weather phenomena in the world; belong to the category of extremely hazardous weather events. Their landfalls can cause human fatalities, structural damages and economic losses worldwide (Manganello *et al*., 2012; Pielke and Pielke, 1997; Simpson *et al*., 2002). They are basically large-scale rotary storms that form over warm ocean waters in the tropical regions (Montgomery and Farrell, 1993). India is mostly affected by the cyclones which develop in the Bay of Bengal (BoB) and the Arabian Sea in the pre-monsoon and post-monsoon seasons. These cyclones basically move west-northwestwards to northwestwards (Chinchole and Mohapatra, 2017). The average life period of these cyclones is 4-6 days (Kumar *et al*., 2017). The average frequencies of these cyclones over BoB and the Arabian Sea are 4 and 1 respectively (Mohapatra *et al*., 2014b). An early prediction about the genesis, development and track of these systems can save many lives.

According to the scientists, tropical cyclones mainly develop over the warm ocean with surface temperatures (SSTs) above 26 °C (Palmen, 1948), decreased vertical shear of horizontal wind (Gray, 1968), enhanced low-level moisture content and increased latent and sensible heat fluxes from the sea surface to the marine boundary layer. Many scientists have also argued that genesis and development of tropical cyclones depend on nearly classic baroclinicity (Bosart and Bartlo, 1991), the interaction of easterly waves or other low-level disturbances with tropical upper tropospheric disturbances (Ramage, 1959; Sadler, 1976; Montgomery and Farrell, 1993), Rossby wave energy dispersion of a preexisting typhoon

(Li and Fu, 2006), the pre-existing mid-tropospheric vortex that forms in radiative-convective equilibrium (Wang *et al*., 2019), easterly wave and Madden Jullian Oscillation (Sanap *et al*., 2020). This shows that the genesis and development process of tropical cyclones is very complex and depends on many factors.

Recently Super Cyclone Amphan which originated in the BoB caused serious destructions in the coastal states West Bengal, Odisha of India. According to the India Meteorological Department (IMD) it was the strongest tropical cyclone to occur in the BoB since 1999 Odisha Super cyclone. The landfall of this cyclone occurred over West Bengal, causing widespread damage. The damages amount to 13 billion USD, which makes it the costliest ever recorded in the North Indian Ocean (NIO) (Poddar *et al*., 2020). It is considered the strongest to hit the region in over a decade killing at least 86 people in West Bengal (Thota *et al*., 2020). In this study, the synoptic and dynamical characteristics that led to the formation and intensification of Super Cyclone Amphan are investigated. In particular, the impact of synoptic-scale factors such as upper level Sub-Tropical Westerly Jet (STWJ), westerly trough and dynamical factors such as surface energy fluxes, CAPE, total column liquid water content, total column rainwater content, SST, wind shear, divergence, the vertical integral of total energy, GPP are analyzed.

2. Study area and data

The study area under consideration is basically India and North Indian Ocean (NIO) region spanning between (10° S-41° N and 50° E-110° E) with particular focus on BoB region (10° S-31° N and 80° E-110° E). Hourly 0.25° × 0.25° resolution European Center for Medium-Range Forecasts (ECMWF) ERA5 reanalysis data (Hersbach and Dee, 2016) for different parameters including wind speed & direction, temperature, vertical velocity, divergence, specific humidity, geopotential and potential vorticity at different pressure levels, Mean Sea Level Pressure (MSLP), Sea Surface Temperature (SST), surface latent heat flux, surface sensible heat flux, the vertical integral of thermal energy, CAPE, column rain water content, column liquid water content, 850 hPa relative vorticity, 24 hours rainfall, 10 m wind and 1000 hPa specific humidity have been utilized in this study for Super Cyclone Amphan (Amphan 12 May, 2020-20 May, 2020). Best track data of super cyclone Amphan have been collected from RSMC New Delhi.

3. Description of life period

According to IMD on 13th May, 2020, an area of low pressure developed over the southeastern Bay of Bengal (BoB) about 1020 km southeast of Visakhapatnam in the Indian state of Andhra Pradesh. In the next few days, the system gradually intensified and became more marked. On 16th May, 2020 0000 UTC the system became a depression while it was located about 1100 km to the south of Paradip, Odisha. Six hours later the system upgraded to a deep depression. This deep depression started moving northwards, continually organized and further strengthened to become a cyclonic storm and received the name Amphan. On 17th May Amphan underwent rapid intensification and transformed into a severe cyclonic storm with winds ranging 140-210 km/h. These winds are equivalent to a Category 4 hurricane on the Saffir-Simpson scale (Simpson and Saffir, 1974). After a few hours, it further intensified to become an extremely severe cyclonic storm. Amphan further strengthened and became Super cyclone on 0600 UTC 18th May. It was in the same category till 0300 UTC 19th May. According to IMD Amphan reached its peak intensity around 1200 UTC 18th May with a 3-minute sustained wind speed of 240 km/h and a minimum central pressure of 925 hPa. The super cyclonic storm continuously moved northeastwards and around 20th May, 1200 UTC it made landfall near Bakkhali, West Bengal (India) as a very severe cyclonic storm. It moved further inland and rapidly weakened. Track of Amphan (from the category of depression) is shown in Fig. 1.

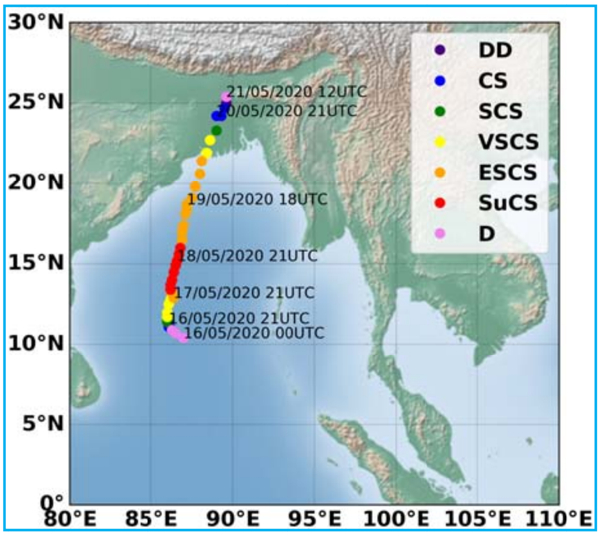

Fig. 1. Track of Super Cyclone Amphan

4. Brief description of important parameters

4.1. *Sub-Tropical Westerly Jet (STWJ)*

According to WMO, a jet stream is a strong narrow current concentrated along a quasi horizontal axis in the upper troposphere or in the stratosphere characterized by strong vertical and lateral wind shears featuring one or more velocity maxima. STWJ is one of the most important jet streams and the mean position of this jet stream over Indian sub-continent is at 27° N at height of about 12 kms (200 hPa). This jet is caused by the concentration of the horizontal temperature gradient below the jet level and the reversal of the gradient above the jet level. This is a large scale feature of the upper air circulation with a high-speed core which can be distinguished from the general wind current. This jet is located near the poleward boundary of the Hadley cell. There is a downstream strengthening of the wind speed in this jet stream. This is seen from Jodhpur to Guwahati across India. The jet continues further north-eastwards across China and Japan with core speeds increasing progressively reaching maximum over south Japan. It is seen that in association with the high-speed centres along the jet axis there is upper air divergence in the left entrance and right exit sectors.

To find the jet 200 hPa wind has been plotted.

4.2. *Wind shear*

The speed and direction of the wind are different in different heights (pressure level). Generally, wind speed increases with height. Vertical shear of the horizontal wind is calculated by using shear = velocity of wind at the upper level – velocity of wind at a lower level. Here wind shear between 200 to 1000 hPa has been taken into consideration.

4.3. *Divergence*

This parameter is the horizontal divergence of velocity. It is the rate at which air is spreading out horizontally from a point, per square meter. This parameter is positive for air that is spreading out, or diverging and negative for the opposite, for air that is concentrating or converging (convergence). 200 hPa mean divergence of all synoptic hours for each day has been shown here.

4.4. *Vertical velocity (ω)*

This parameter is the speed of air motion in the upward or downward direction. Negative values of vertical velocity indicate upward motion. It can be expressed as:

$$\omega = -\frac{dp}{dt} \quad (1)$$

where, $\frac{dp}{dt}$ is the rate of change of pressure.

4.5. *CAPE*

This is an indication of the instability (stability) of the atmosphere and can be used to assess the potential for the development of convection, which can lead to heavy rainfall, thunderstorms and other severe weather. This is the potential energy represented by the total excess buoyancy. The larger positive CAPE value indicates larger instability.

4.6. *Surface heat fluxes*

Surface latent heat flux is the transfer of latent heat (resulting from water phase changes, such as evaporation and condensation) between the Earth’s surface and the atmosphere through the effects of turbulent air motion. Surface sensible heat flux is the transfer of heat (excluding latent heat) between the Earth’s surface and the atmosphere through the effects of turbulent air motion. The magnitude of sensible heat flux is governed by the difference in temperature between the surface and overlying atmosphere, wind speed and surface roughness. Surface heat fluxes are positive downwards and negative upwards.

4.7. *Column rainwater and liquid water content*

Total column rainwater is the total amount of water in droplets of raindrop size (which can fall to the surface as precipitation) in a column extending from the surface of the Earth to the top of the atmosphere. Total column liquid water content is the amount of liquid water contained within cloud droplets in a column extending from the surface of the Earth to the top of the atmosphere. Rain droplets which are much larger in size (and mass) are not included in this parameter.

4.8. *Vertical integral of total energy*

This is the vertical integral of total energy for a column of air extending from the surface of the Earth to the top of the atmosphere. Total atmospheric energy is made up of internal, potential, kinetic and latent energy. This is measured in Joule/m^2.

4.9. *Upper-level trough*

The trough is an elongated region of relatively low atmospheric pressure without a closed isobaric contour that would define it as a low-pressure area. The trough may be near the surface or aloft. Upper-level troughs reflect cyclonic filaments of vorticity. Their motion induces upper-level wind divergence. Their interaction with a cyclonic system can influence and guide the system. The trough at a particular level can be found out by plotting the geopotential at that particular level.

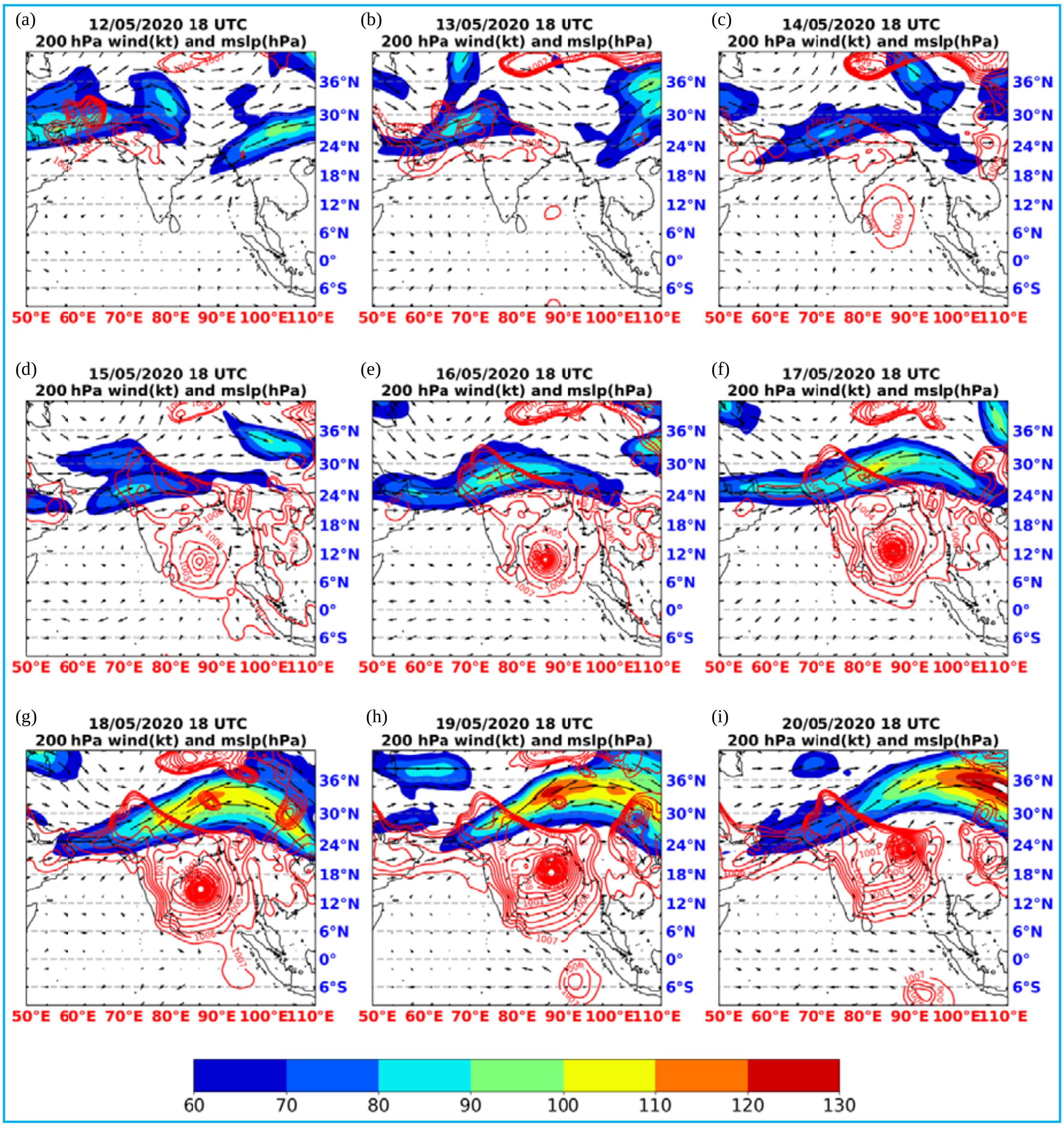

Figs. 2(a-i). Sub-Tropical Westerly Jet (STWJ) and Mean Sea Level Pressure (MSLP)

4.10. *Relative vorticity and potential vorticity*

This parameter is the measure of the rotation in the horizontal, around a vertical axis, relative to a fixed point on the surface of the earth. A positive value of this parameter is associated with the weathers which show anticlockwise rotation in the northern hemisphere. Potential vorticity is a measure of the capacity for air to rotate in the atmosphere. If we ignore the effects of heating and friction, potential vorticity is conserved following an air parcel. It is used to look for places where large wind storms are likely to originate and develop. 850 hPa mean relative vorticity of all synoptic hours for each day has been shown here.

4.11. *Genesis Potential Parameter (GPP)*

(Kotal *et al.*, 2009) developed a genesis potential parameter (GPP) using the variables relative vorticity

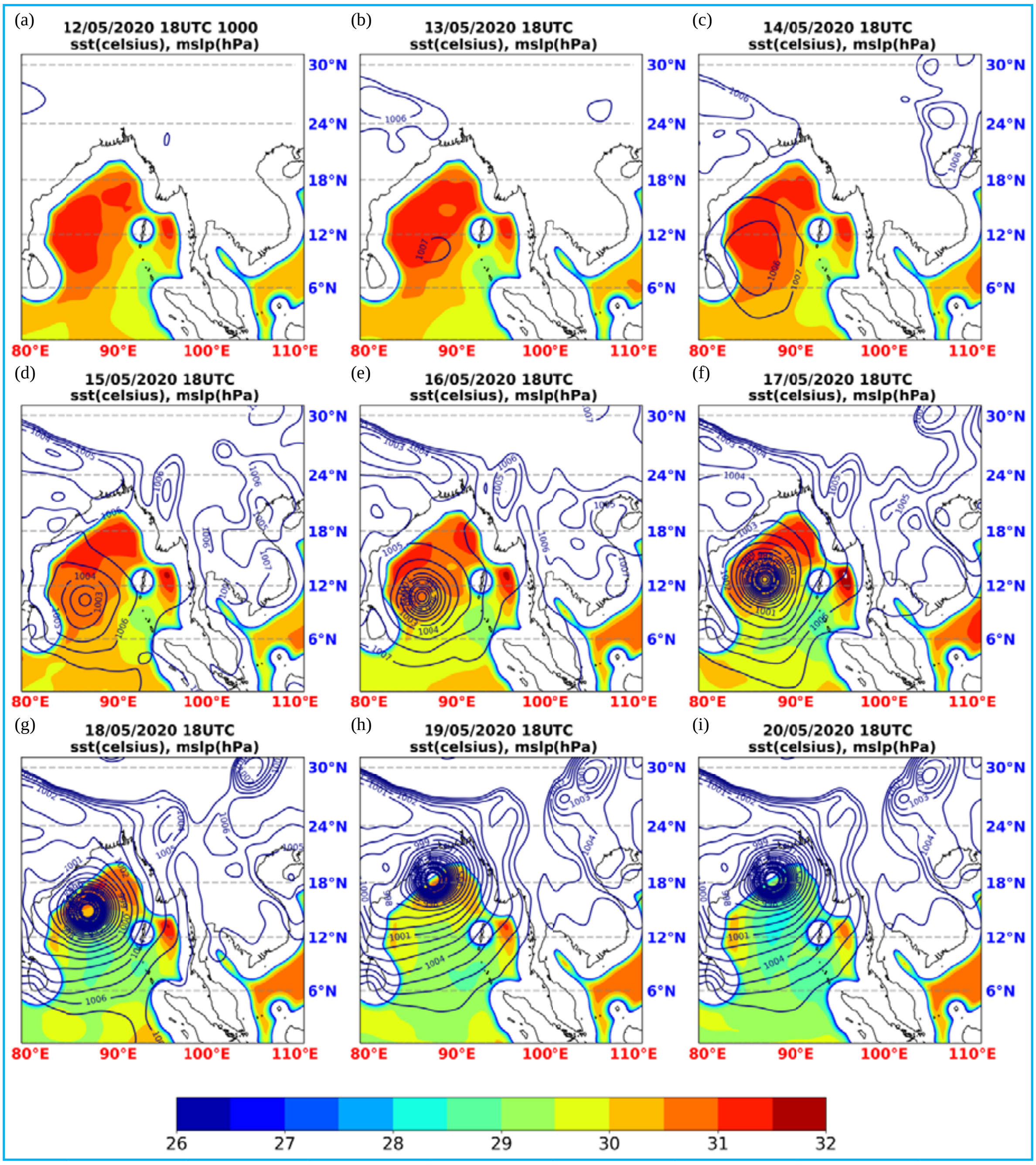

Figs. 3(a-i). Sea Surface Temperature (SST) and Mean Sea Level Pressure (MSLP)

at 850 hPa, middle tropospheric relative humidity, middle tropospheric instability and vertical wind shear variables. The GPP was defined as:

$$\text{GPP} = \frac{M \times I\zeta_{850}}{S} \text{ if } \zeta_{850} > 0, M > 0, I > 0$$

$$= 0 \text{ if } \zeta_{850} \leq 0, M \leq 0, I \leq 0 \qquad (2)$$

where,

ζ_{850} is the relative vorticity at 850 hPa in (10^{-5} s^{-1}).

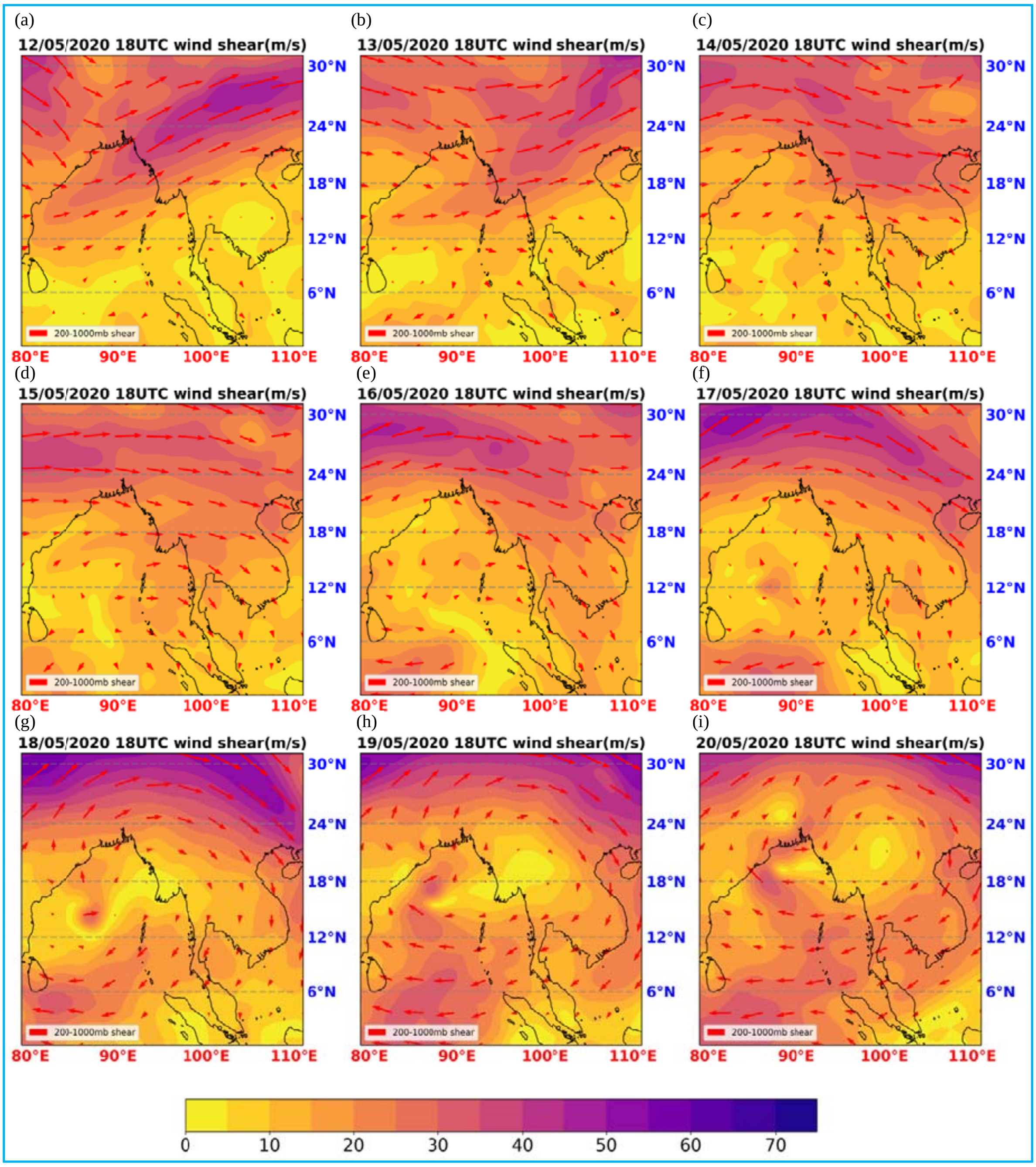

Figs. 4(a-i). Wind shear

S is the vertical shear of the horizontal wind between 200 and 850 hPa (ms^{-1}).

$$M = \frac{(RH - 40)}{30}$$ M is the mid-tropospheric relative humidity.

RH is the mean relative humidity between 700 and 500 hPa.

$I = (T_{850}-T_{500})$ °C = Middle-tropospheric instability (temperature difference between 850 hPa and 500 hPa).

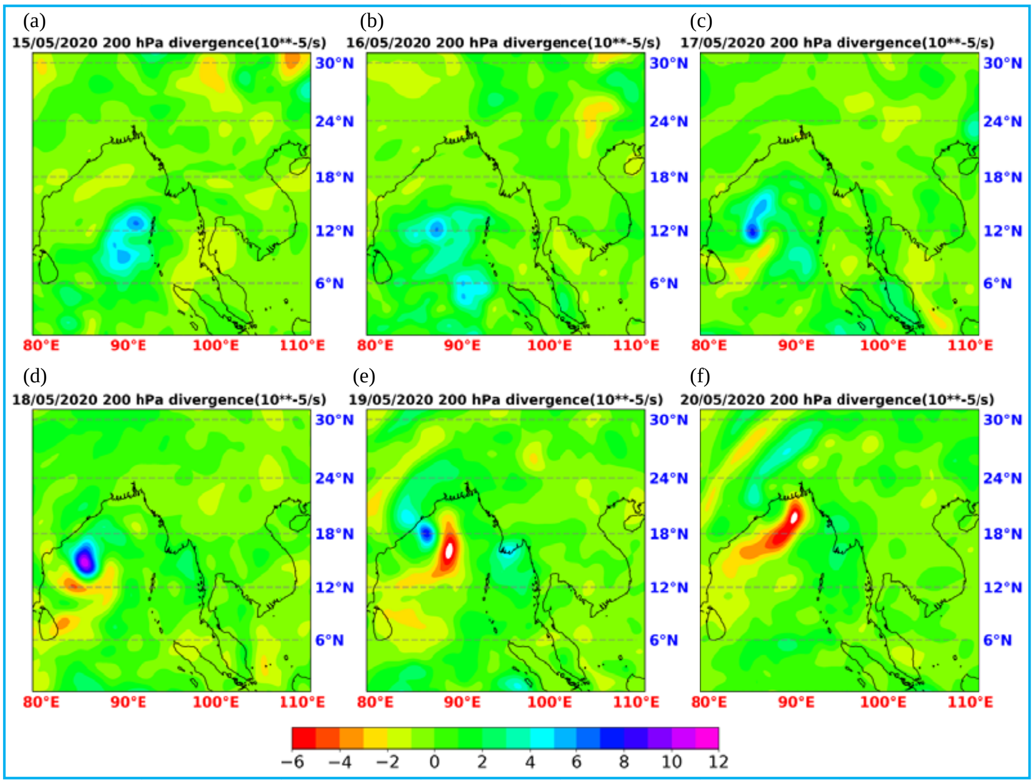

Figs. 5(a-f). 200 hPa divergence

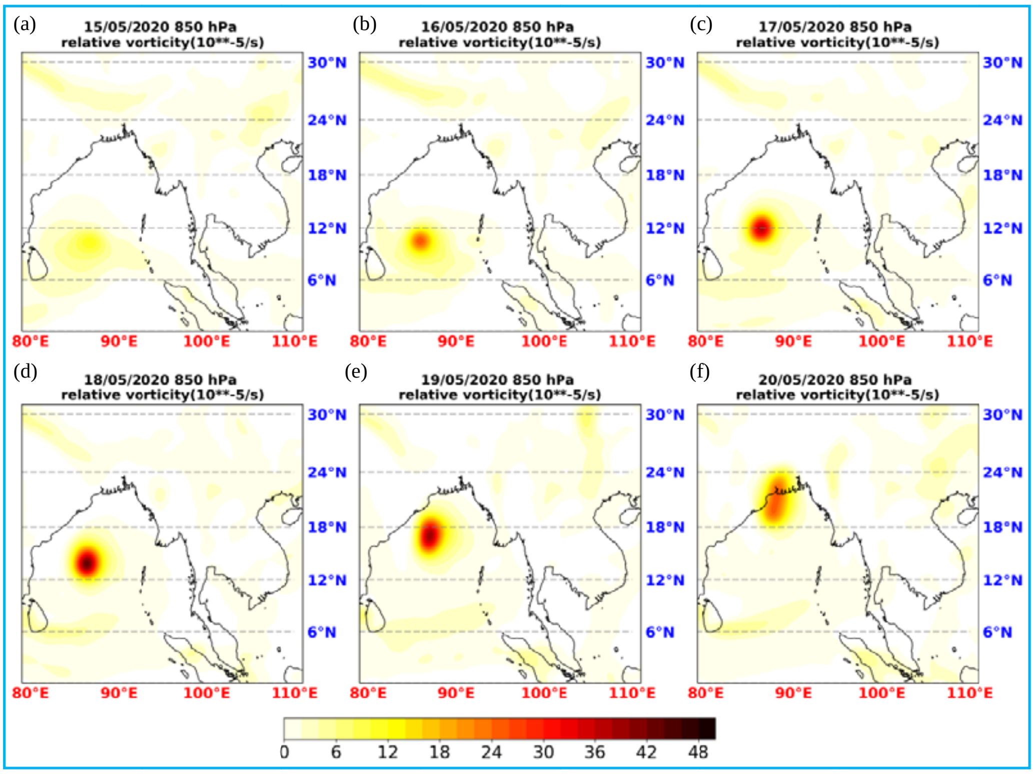

Figs. 6(a-f). 850 hPa relative vorticity

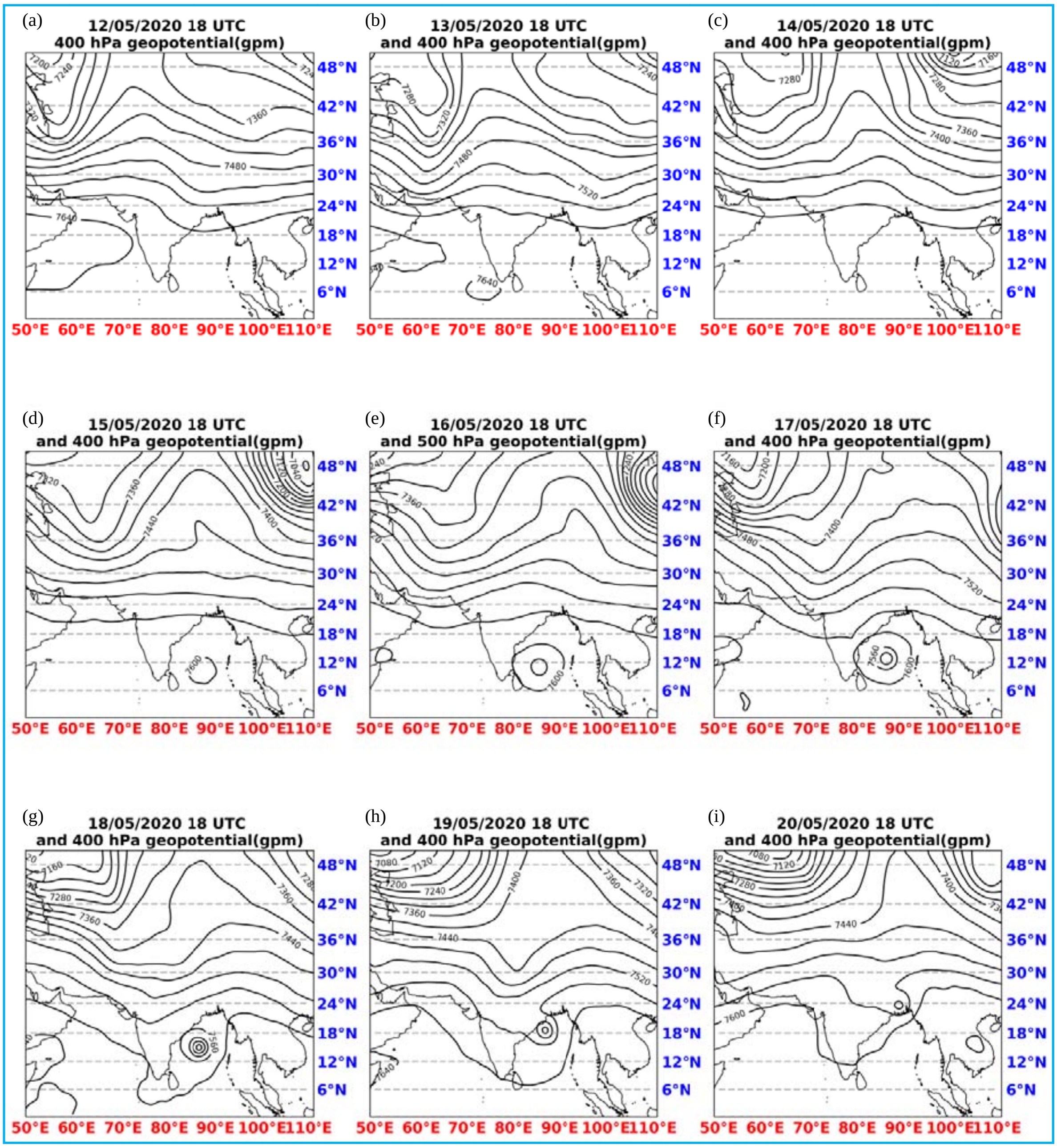

Figs. 7(a-i). 400 hPa geopotential

This is an important predictor for genesis and intensification of tropical cyclone.

5. Synoptic and dynamical conditions

During cyclogenesis tropical cyclones mainly depend on the sea surface heat fluxes and vertical shear of the horizontal wind (De Maria, 1996; Latif *et al*., 2007; Dare and McBride, 2011). High SST plays a crucial role in enhancing deep convection by supplying necessary heat and moisture in the upward direction. At a given latitude the rate of intensification increases with increasing SST, on account of the significant increase of the surface moisture fluxes from the warmer ocean (Črnivec *et al*., 2016). The low wind shear in an unstable stratified atmospheric environment allows the uniform

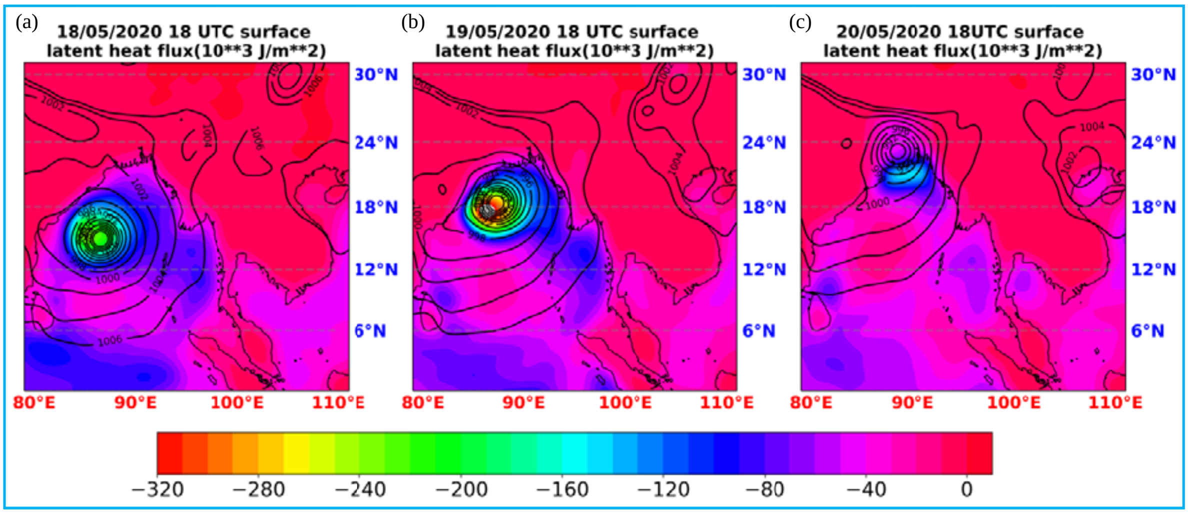

Figs. 8(a-c). Surface latent heat flux

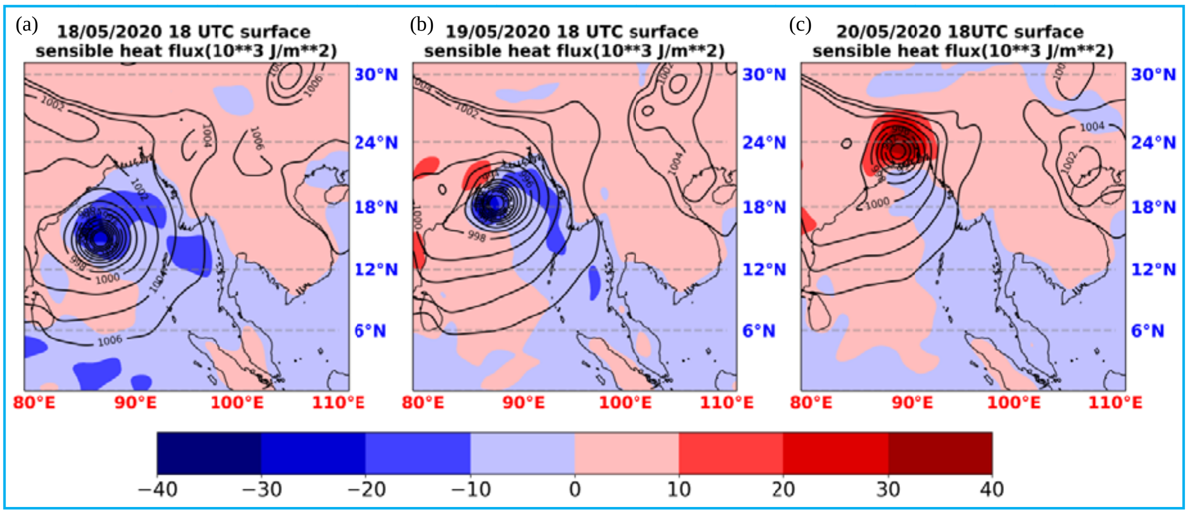

Figs. 9(a-c). Surface sensible heat flux

upward and undisturbed release of the latent heat from the sea surface supporting the upper air supply with moisture and energy. It also contributes to the vertical alignment of the tropical cyclone which helps to keep the system intact and strengthen. Upper-level jet also plays a crucial role ingenesis and development of tropical cyclones. It enhances the divergence in its right exit and left entrance sectors. According to the dines compensation principle this divergence creates lower level convergence. Upper-level divergence aloft the sea surface helps vertical development above the sea surface. With the strengthening of the jet, this vertical development strengthens and pressure falls on the sea surface. Thus upper-level jet helps in the genesis of tropical cyclones. The upper-level westerly trough ridge pattern and jet also intensify and guide the cyclones in its trajectory.

According to IMD during 13th May, 2020, an area of low pressure developed over the Southeastern Bay of Bengal (BoB) about 1020 km southeast of Visakhapatnam in the Indian state of Andhra Pradesh. The spatial patternsof the MSLP and 200 hPa wind depicts the omnipresence of low pressure over southeastern parts of BoB and STWJ in the region (24-40° N, 100-110° E) [Fig. 2(b)]. The area of low pressure was situated in a more favourable region comprising of low vertical shear of horizontal wind, high SST (exceeding 31 °C) [Fig. 3(b)] and high energy [Figs. 10(g-i)]. The combined impact of

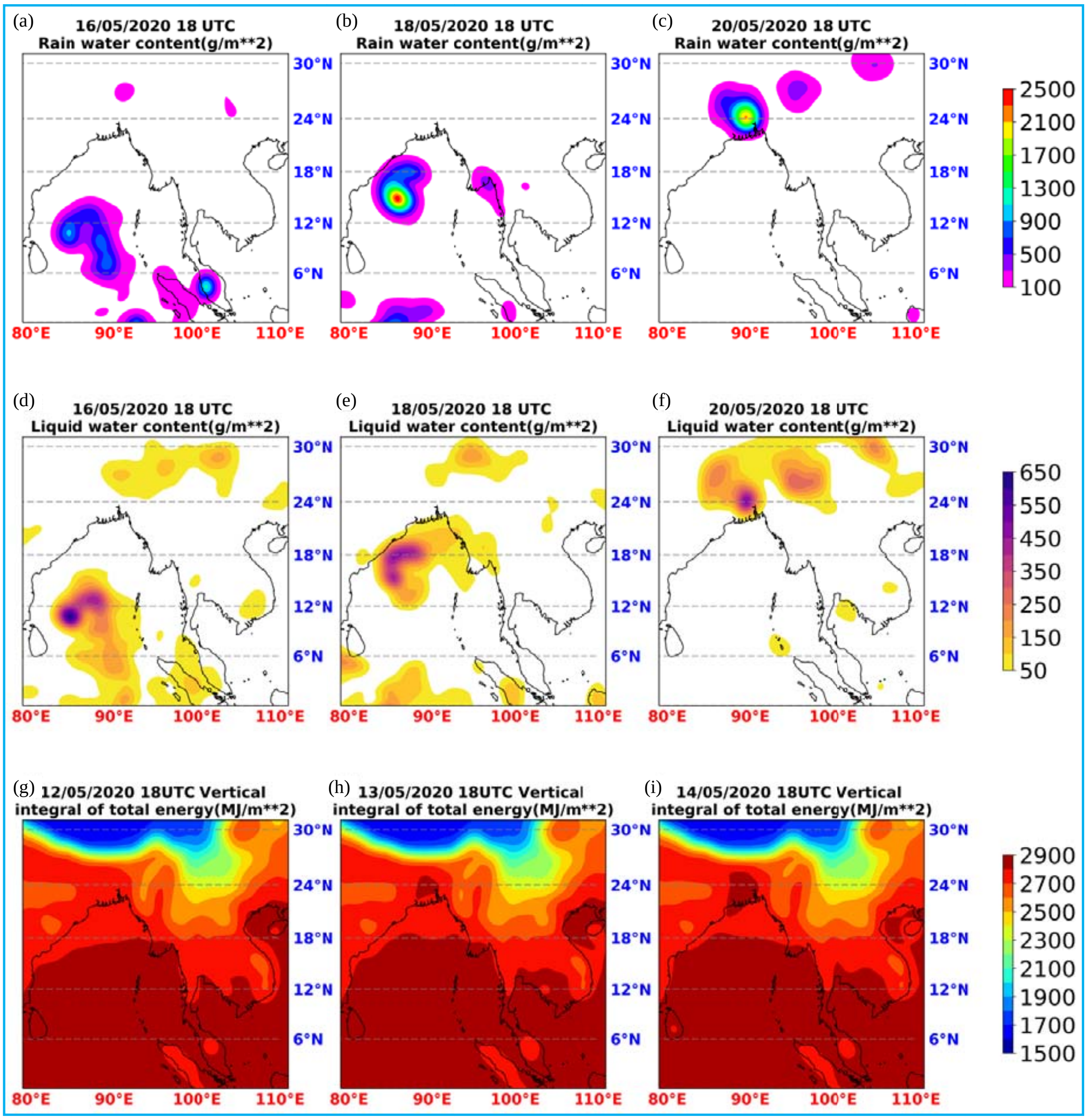

Figs. 10(a-i). Column total rain water content , liquid water content and vertical integral of total energy

high SST [Figs. 3(a-i)] and low vertical shear (<10 m/s) [Figs. 4(a-i)] acts in initiating the conducive environment for the cyclone movement and sustainment. The large temperature gradient between the warm sea surface and colder atmosphere [Fig. 14(c)] increases the heat exchange and enhances the convection. The 200 hPa wind and MSLP in Figs. 2(a-i) show the time evolution of STWJ and the system. It is seen from this figure that with time STWJ strengthens and isobars become closely spaced. This STWJ is associated with upper-level divergence [Figs. 5(a-f)] & lower-level convergence indicated by 850 hPa relative vorticity [Figs. 6(a-f)]. This is also evident from the vertical profile of divergence shown in Fig. 15(b). This existence of the upper-level divergence and lower-level convergence enhances the instability and favours the intensification of the system which is evident from the profile of vertical velocity and potential vorticity [Fig. 14(a&b]. The upper-level divergence and lower level relative vorticity is maximum on 18th May when Amphan becomes Super cyclone [Fig. 5(d), Fig. 6(d)]. The surface wind was at its peak [Fig. 11(a)] and pressure around the eye falls to its minimum. (Hanley *et al*., 2001) examined

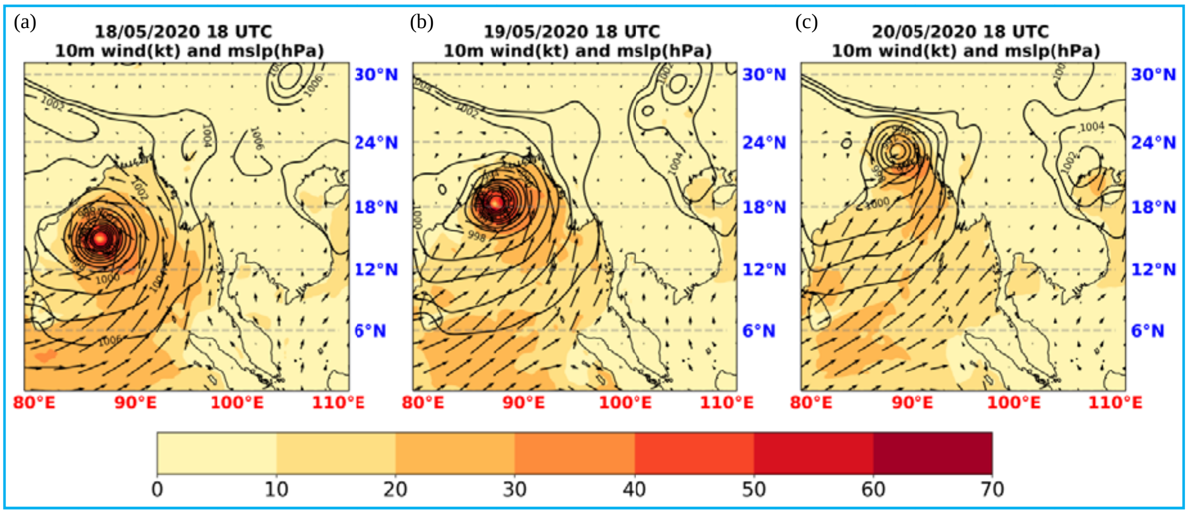

Figs. 11(a-c). 10 m wind and MSLP

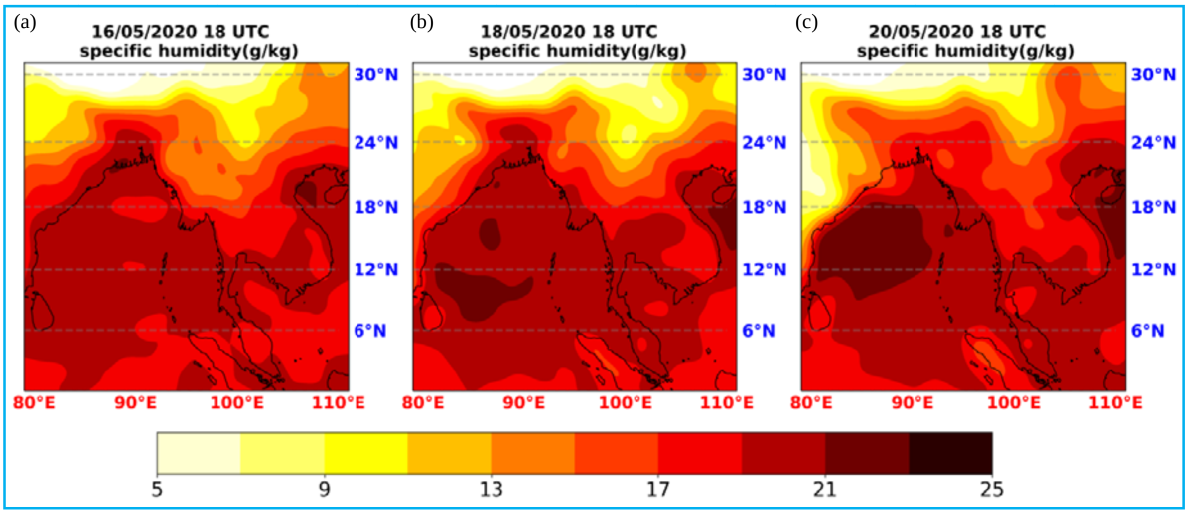

Figs. 12(a-c). 1000 hPa specific humidity

that tropical cyclones over warm water and away from land are more likely to intensify than weaken after an interaction with an upper-level trough. From Fig. 7(a) it is seen that there exist an upper-level westerly trough at 400 hPa in the region (50-60° E). This trough shows an oscillation during 12-16 May [Figs. 7(a-e)] and after that, it shifts meridionally [Figs. 7(f-i)]. This trough starts interacting with the system after 15th May [Figs. 7(e-i)] which may have intensified the system. Vertical wind profile [Fig. 15(a)] shows that wind speed is maximum between 500-300 hPa which confirms the upper-level trough interaction with Amphan. Surface latent heat flux is the transfer of latent heat between Earth's surface (land/ocean) and the atmosphere through the effects of turbulent air motion. Evaporation from the Earth's surface represents a transfer of energy from the surface to the atmosphere. (Emanuel, 1986) proposed that "intensification and maintenance of tropical cyclones depend exclusively on self-induced heat transfer from the ocean" *via* surface heat fluxes. (Wing *et al*., 2019) also argued that strong feedback of surface heat fluxes such as surface latent heat flux and surface sensible heat flux can intensify tropical cyclones. (Chen *et al*., 2014) stated that latent heat flux exchanges at the air-sea interface play important roles in the formation and development of tropical cyclones. It is the fundamental source of energy of tropical cyclones (Ma *et al*., 2015). Figs. 8(a-c) show the surface latent heat flux during 18-20 May. Fig. 8(a) shows that strong and negative latent heat flux at the centre of Amphan. This may suggest that Amphan is still

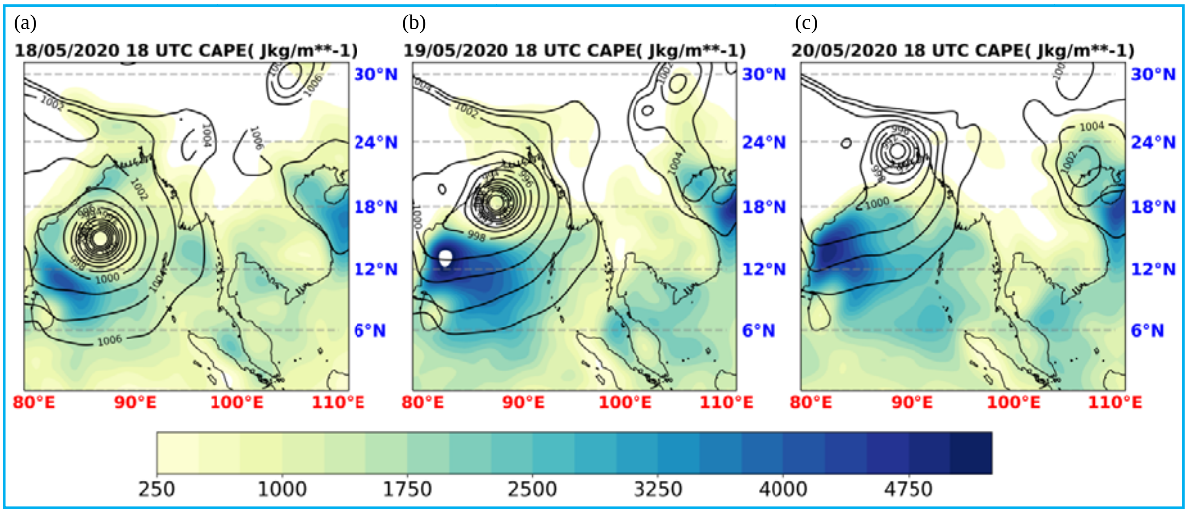

Figs. 13(a-c). CAPE

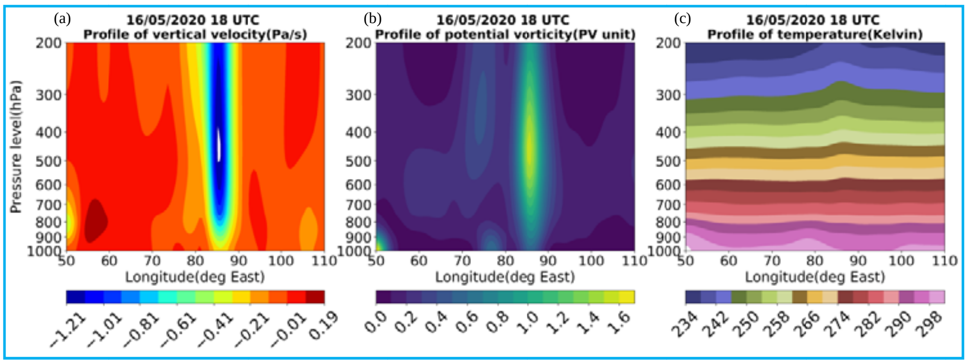

Figs. 14(a-c). Vertical velocity, potential vorticity and temperature profile

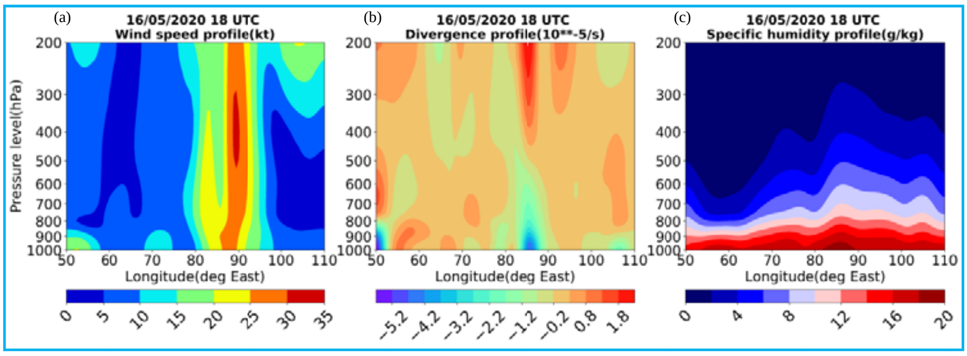

Figs. 15(a-c). Wind speed, divergence and specific humidity profile

developing by consuming the latent energy from the underlying ocean *via* latent heat flux (Malkus and Reihl, 1960) and also from latent energy released due to codensation of water vapour. It also suggests that the strong vertical development by condensing the water vapour into the super cooled ice-water mixture at the top and liquid water. That means more precipitable/rainwater at this stage, which is evident from Figs. 10(b-e). The local rate of supply of heat energy (primarily latent heat) from the ocean increases with increasing surface wind speed [Figs. 11(a-c)] (Zhu *et al.*, 2004). Latent heat flux is maximum on 19th May [Fig. 8(b)] when Amphan was at

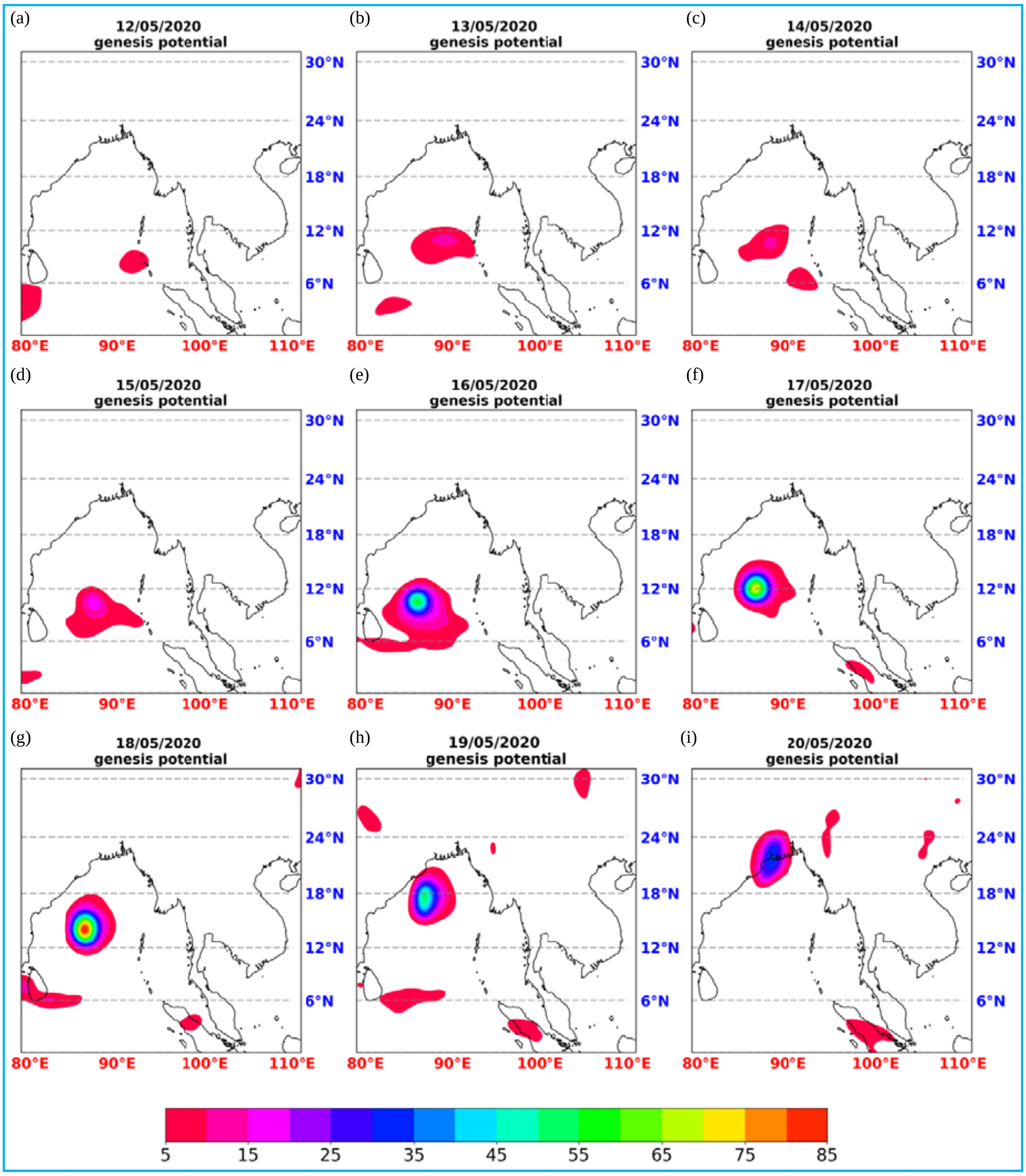

Figs. 16(a-i). Evolution of genesis potential parameter for Super Cyclone Amphan

the category of Supercyclone. The surafce wind speed was high [Fig. 11(b)] and surface pressure around the eye was also near to minimum. After that, the latent heat flux & surface wind speed reduced [Fig. 8(c), Fig. 11(c)]. This suggests the decrease of pressure around the eye of Amphan causes the winds to increase which in turn increases the rate of evaporation and acts as positive feedback to Amphan's intensification. Maximum latent heat flux is associated with maximum total column rain/liquid water in Amphan [Figs. 10(b-e)]. After landfall Amphan brings heavy precipitation which reduces its rain/ liquid water content [Figs. 10(c-f)]. Surface sensible heat flux is the transfer of heat between the Earth's surface and the atmosphere through the effects of turbulent air motion

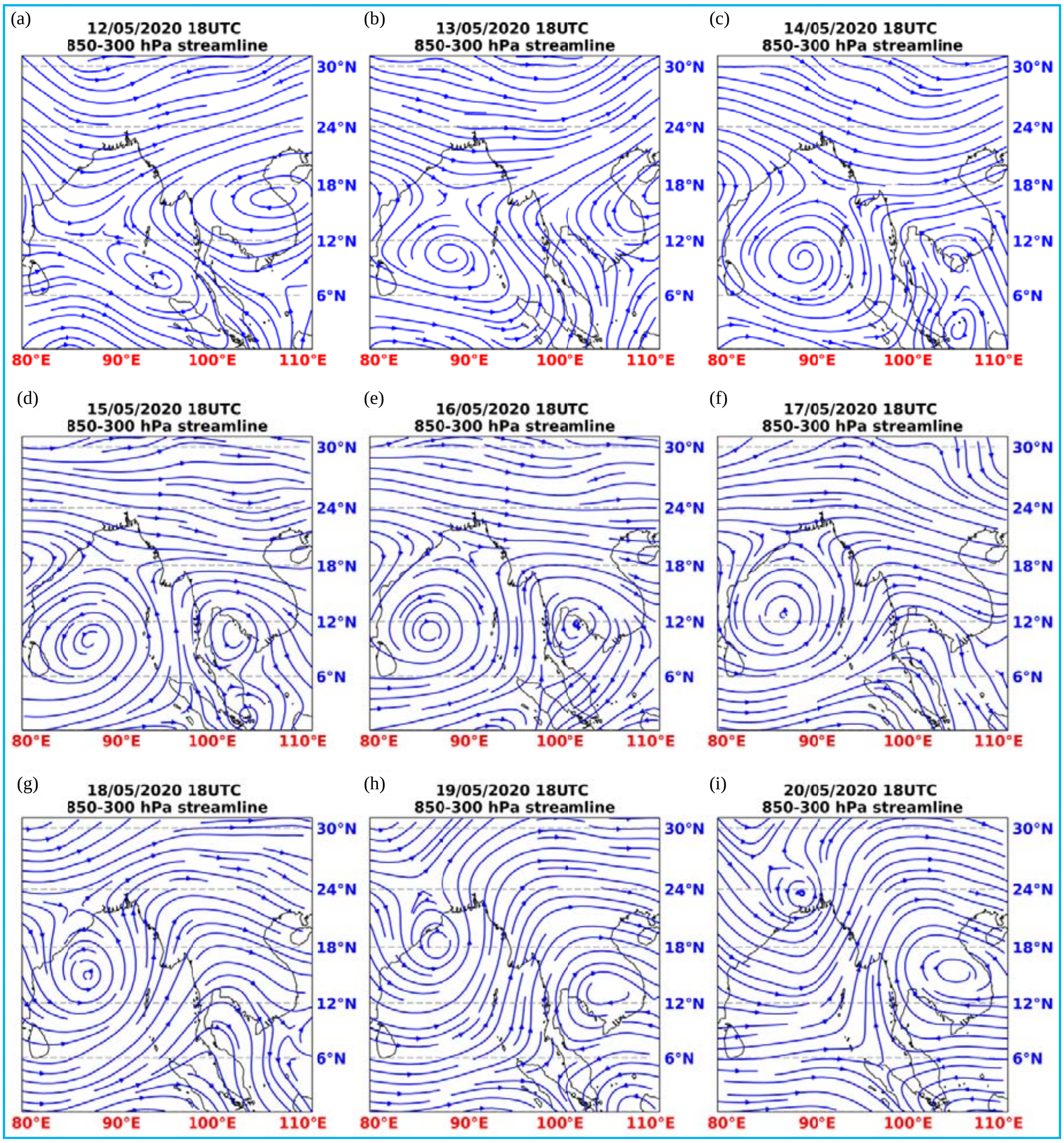

Figs. 17(a-i). 850-300 hPa streamline

(but excluding any heat transfer resulting from condensation or evaporation). The magnitude of the sensible heat flux is governed by the difference in temperature between the surface and the overlying atmosphere, wind speed and surface roughness. Though the impact of surface sensible heat flux on the tropical cyclone intensification is not distinct, (Ma *et al*., 2015) showed that the size of a tropical cyclone is influenced by it. It is crucial for the growth of outer rainbands. Figs. 9(a-c) show the surface sensible heat flux during 18-20 May. Surface sensible heat flux has effects of warming the near-surface air directly (Ma, 2018). From Fig. 9(c) it is seen that after landfall the value of surface sensible heat flux is maximum. This explains the turning of trees into yellow and red at the area landfall. Low level (1000 hPa) moisture supply as shown in Figs. 12(a-c) also played an important role in enhancing Amphan's instability. Vertical profile of specific humidity shown in Fig. 15(c) shows the abundance of moisture around the cyclone with the maximum around the eye. As depicted in Figs. 12(a-c). moisture supply from the south-west (specific humidity > 20 g/kg) sustains the moisture content of the system and enhances the low-level convection. Moreover, the horizontal distribution of the convective available potential energy (CAPE) indicates that the areas of high CAPE around Amphan are collocated with the areas of abundant amount of surface moisture content. (Lee *et al*., 2018) observed that tropical cyclone intensification rate increases with increasing CAPE and inner core CAPE are smaller than that of the ambient region [Figs. 13(a-c)]. They also found a positive relationship between radial CAPE gradient and the intensification rate. Fig. 13(b) shows that on 19th May 1800 UTC, CAPE exceeds 5250 Jkgm^{-1} at the south-west sector of Amphan. The upper-level jet, steering flow (averaged wind fields between 850-300 hPa to incorporate the effect upper-level trough ridge) guides Amphan in its trajectory till landfall on the West Bengal coast [Fig. 17(a-i)]. Amphan causes heavy rainfall and high surface winds [Figs. 11(a-c)] near the area of landfall fall which caused severe destruction.

GPP which is described in subsection 4.11 has been calculated using equation 2 and its daily evolution is shown in Figs. 16(a-i). It is seen that there is a gradual increase in GPP. The GPP value above 30 (threshold by Kotal *et al*., 2009) is seen from 16th May onwards. From 45 on 16th May, it abruptly reaches to 75 on 17th May. As discussed earlier Amphan underwent rapid intensification on 17th May. The minimum value of GPP around 10 is seen on 12th May and the value reaches to a maximum around 85 on 18th May. On this day Amphan reached its maximum intensity and transformed into a super cyclone. Therefore the maximum value of GPP occurs when Amphan reaches its maximum intensity.

As stated in Section 3, on 17th May Amphan underwent rapid intensification and transformed into a severe cyclonic storm with winds ranging 140-210 km/h. At a given latitude the rate of intensification increases with increasing SST. (Sanap *et al*., 2020) showed that the region of high SST coincides with the region of rapid intensification in the case of cyclone Ockhi. From Fig. 3(f), it is clear that SST was abnormally high (32 °C) on 17th May. In addition to this other factors such as low shear [Fig. 4(f)], high upper-level divergence [Fig. 5(c)] and lower level vorticity [Fig. 6(c)] may be the reason behind this rapid intensification. Before the landfall Amphan weakened and became an extremely severe cyclonic storm. The reason may be reduced upper-level divergence [Fig. 5(f)], low lower-level convergence [Fig. 6(f)], low SST [Fig. 3(i)] and low surface latent heat flux [Fig. 8(c)].

6. Conclusions

The main objective of this study is to find out the synoptic and dynamical conditions that led to the genesis and intensification of tropical cyclone Amphan. The synoptic and dynamical conditions associated with Amphan have been discussed thoroughly in section 5. From this, it can be concluded that under favourable conditions of high SST, high energy and weak vertical shear of horizontal wind, the 200 hPa STWJ has helped in the genesis of Amphan. The weak vertical shear, high SST, high-temperature gradient between warmer sea surface & colder atmosphere and strong upper-level divergence have increased the heat and moisture exchange between the sea surface and the atmosphere via surface heat fluxes and vertical winds. These have enhanced convection and intensified the system. The interaction of 400 hPa trough with Amphan has also intensified it. Abnormally high SST (on 17th May) and combined effect of strong upper-level divergence, lower level convergence and low wind shear may be the reason behind the rapid intensification of Amphan. The 400 hPa trough and upper-level jet have guided Amphan in its trajectory.

Acknowledgements

I gratefully acknowledge India Meteorological Department for encouraging and supporting me to do this study. The contents and views expressed in this paper are the views of the authors and do not necessarily reflect the views of the organization they belong to.

Acronyms

STWJ	:	Sub Tropical Westerly Jet
CAPE	:	Convective Available Potential Energy
SST	:	Sea Surface Temperature
MSLP	:	Mean Sea Level Pressure
BoB	:	Bay of Bengal
NIO	:	North Indian Ocean
ECMWF	:	European Center for Medium Range Forecasts
IMD	:	India Meteorological Department
GPP	:	Genesis Potential Parameter

References

Bosart, L. F. and Bartlo, J. A., 1991, "Tropical storm formation in a baroclinic environment", *Mon. Wea. Rev.*, **119**, 1979-2013.

Chen, S., Li, Weibiao., Lu, Youyu and Wen, Z., 2014, "Variations of latent heat flux during tropical cyclones over the South China Sea", *Meteorol. Appl.*, **21**, 717-723.

Chinchole, P. S. and Mohapatra, M., 2017, "Some characteristics of Transitional Speed of Cyclonic Disturbances Over north Indian Ocean in Recent Years, *Tropical Cyclone activity over the North Indian Ocean*, Ed. Mohapatra, M., Bandyopadhyay, B. K. and Rathore, L. S., Co-published by Capital Publishers, New Delhi and Springer, Germany, 165-179.

Čranivec, N., Smith, R. K. and Gerard, Kilroy, 2016, "Dependence of tropical cyclone intensification rate on sea-surface temperature", *Q. J. R. Meteorol. Soc.*, **142**, 1618-1627.

Dare, R. A. and Mc Bride, J. L., 2011, "The sea surface temperature condition for tropical cyclogenesis", *J. Climate.*, **24**, 4570-4576.

De Maria, M., 1996, "The effect of vertical shear on tropical cyclone intensity change", *J. Atmos. Sci.*, **53**, 2076-2087.

Emanuel, K. A., 1986, "An air-sea interaction theory for tropical cyclones. Part I : Steady-state maintenance", *J. Atmos. Sci.*, **43**, 585-605.

Gray, W. M., 1968, "Global view of the origin of tropical disturbances and storms", *Mon. Wea. Rev.*, **96**, 669-700.

Hanley, D., Molinary, J. and Keyser, D., 2001, "A composite study of the interactions between tropical cyclones and upper-tropospheric troughs", *Mon. Wea. Rev.*, **129**, 2570-2584.

Hersbach, H. and Dee, D., 2016, "ERA5 reanalysis is in production", *ECMWF Newslett.*, **147**, 7.

Kotal, S. D., Kundu, P. K. and Roy Bhowmik, S. K., 2009, "An analysis of cyclogenesis parameter for developing and non developing low pressure systems over the Indian Sea", *Nat. Hazards*, **50**, 389-402.

Kumar, S. V. J., Ashthikar, S. S. and Mohapatra, M., 2017, "Life Period of Cyclonic Disturbances Over the North Indian Ocean During Recent Years", In : *Tropical Cyclone Activity over North Indian Ocean*, Ed. Mohapatra, M., Bandyopadhyay, B.K. and Rathore, L.S., Co-published by Capital Publishers, New Delhi and Springer, Germany, 181-198.

Latif, M., Keenlyside, N. and Brader, J., 2007, "Tropical sea surface temperature, vertical wind shear and hurricane development", *Geophys. Res. Lett.*, https://doi.org/10.1029/2006GL027969.

Lee, M. and Frisius, T., 2018, "On the role of convective available potential energy (CAPE) in tropical cyclone intensification", *Tellus A*, **70**, 1433433.

Li, T. and Fu, B., 2006, "Tropical Cyclogenesis Associated with Rossby Wave Energy Dispersion of a Preexisting Typhoon. Part I : Satellite Data Analysis", *J. Atmos. Sci.*, **63**, 1377-1389.

Ma, Z., 2018, "Examining the contribution of surface sensible heat flux induced sensible heating to tropical cyclone intensification from balance dynamics theory", *Dynamics of atmosphere and oceans*, **84**, 33-45.

Ma, Z., Fei, J., Huang, X. and Cheng, X., 2015, "Contributions of surface sensible heat fluxes to tropical cyclone. Part I: Evolution of Tropical cyclone intensity and structure", *J. Atmos. Sci.*, **72**, 120-140.

Malkus, J. S. and Reihl, H., 1960, "On the dynamics and energy transformations in steady-state hurricane" *Tellus*, **12**, 1-20.

Manganello, J. V., K. I., Hodges, Kinter, J. L. III., Cash, B. A., Marx, L., Jung, T., Achuthavarier, D., Adams, J. M., Altshuler, E. L., Huang, B., Jin, E. K., Stan, C., Towers, P. and Wedi, N., 2012, "Tropical cyclone climatology in a 10-km global atmospheric GCM : toward weather-resolving climate modeling", *J. Clim.*, **25**, 11, 3867-3893.

Mohapatra, M., Bandyopadhyay, B. K., Ray, Kamaljit and Rathore, L. S., 2014b, "Early Warning Services for Management of Cyclones over North Indian Ocean : Current status and future scope, High Impact Weather Events over SAARC Region", Ed. Ray, Kamaljit, Mohapatra, M., Bandyopadhyay, B. K. and Rathore, L. S., Capital Publishing Co. and Springer Publications Ltd.

Montgomery, M. T. and Farrell, B. F., 1993, "Tropical Cyclone Formation", *J. Atmos. Sci.*, **50**, 285-310.

Palmén, E., 1948, "On the formation and structure of tropical hurricanes", *Geophysica*, **3**, 26-39.

Pielke, R. A. and Pielke, R. A. S., 1997, "Hurricanes : Their Nature and Impacts on Society", John Wiley and Sons, p279.

Poddar, S., Mondal, M. and Ghosh, S., 2020, "A Survey on Disaster: Understanding the After effects of Super Cyclone Amphan and Helping Hand of Social Media", *arXiv*, arXiv : 2007. 14910v1[cs.CY] 29th July, 2020.

Ramage, C. S., 1959, "Hurricane development", *J. Meteorol.*, **16**, 227-237.

Sadler, J. C., 1976, "A role of the tropical upper tropospheric trough in early season typhoon development", *Mon. Wea. Rev.*, **104**, 1266-1278.

Sanap, S. D., Mohapatra, M., Ali, M. M., Priya, P. and Varaprasad, D., 2020, "On the dynamics of cyclogenesis, rapid intensification and recurvature of the very severe cyclonic storm, Ockhi", *J. Earth., Syst. Sci.*, **129**, p194.

Simpson, R. H. and Saffir, H., 1974, "The hurricane disaster potential scale", *Weatherwise*, **27**, 8, p169.

Simpson, R., Anthes, R. A. and Garstang, M., 2002, "Hurricane! Coping with Disaster : Progress and Challenges since Galveston", *Amer. Geophys. Union*, p360.

Thota, S. M., Kumar, S., Dube, A., Karunasagar, S., Singh, H., Indira Rani S., Kumar, S., Amar Jyothi, K., Sarkar, A., Prasad, S. K., Chakraborty, P., Momin, I. M., Arulalan, T., Preveen Kumar, D., Ashrit, R. and Rajagopal, E. N., 2020, "Super Cyclone "Amphan" : Verification of NCMRWF Model Forecasts", *Research Report*, NMRF/RR/01/2020.

Wang, Y., Davis, C. A. and Huang, Y., 2019, "Dynamics of Lower-Tropospheric Vorticity in Idealized Simulations of Tropical Cyclone Formation", *J. Atmos. Sci.*, **76**, 707-727.

Wing, A. A., Camargo, S. J., Sobel, A. H., Kim, D., Moon, Y., Murakami, H., Reed, K. A., Vecchi, G. A., Wehner, M.F., Zarzycki, C. and Zhao, M., 2019, "Moist static energy budget analysis of tropical cyclone intensification in high resolution climate models", *J. Clim.*, **32**, 6071-6095.

Zhu, H., Ulrich, W. and Smith, R. K., 2004, "Ocean effects on tropical cyclone intensification and inner-core asymmetries", *J. Atmos. Sci.*, **61**, 1245-1258.